

Article

# Multijetfusion Manufacturing Parameters for Watertightness, Strength and Tolerances

Sergio Morales-Planas<sup>1,2</sup>, Joaquim Minguella-Canela<sup>2</sup>, Jordi Lluma-Fuentes<sup>2</sup>, J. Antonio Travieso-Rodriguez<sup>2</sup> and Andrés-Amador García-Granada<sup>3,\*</sup>

<sup>1</sup> Fluidra, Av. de Francesc Macià, 60, 08208 Sabadell, Barcelona; smorales@fluidra.com

<sup>2</sup> UPC, Av. Eduard Maristany, 16, 08019 Barcelona; joaquim.minguella@upc.edu, jordi.lluma@upc.edu, antonio.travieso@upc.edu

\* GEPI-IQS-URL, Via Augusta, 390, 08017 Barcelona; andres.garcia@iqs.edu; Tel.: +34-678-531-783

**Abstract:** The aim of this paper is to explore the watertightness behaviour for high pressure applications using Multijetfusion technology and polyamide 12 as a material. It reports an efficient solution for manufacturing functional prototypes and final parts for water pressure applications. It provides manufacturing rules to engineers in the pressurized product development process up to 10 MPa of nominal pressure. The research findings show manufacturers the possibility of using additive manufacturing as an alternative to traditional manufacturing. Water leakage was studied using different printing orientations and wall thickness for a range of pressure values. An industrial ball valve was printed and validated with the ISO 9393 standard also meeting tolerance requirements. This paper is a pioneering approach to the additive manufacturing of high performance fluid handling components. This approach solves the problem of leakage caused by porosity in additive manufacturing technologies.

**Keywords:** keyword 1; keyword 2; keyword 3 (List three to ten pertinent keywords specific to the article; yet reasonably common within the subject discipline.)

---

## 1. Introduction

Additive manufacturing, also known as 3D printing, converts a computer-aided three-dimensional model (CAD) to a physical object without the need of moulds or tooling. It transforms the manufacturing method from analogical to digital [1]. The manufacturing process is based on the addition of material combined with a contribution of energy to create a solid, layer by layer. Additive technologies lead to new manufacturing paradigms such as decentralized manufacturing or mass customization. However, the transition from Rapid Prototyping (RP) to Additive Manufacturing (AM) entails new challenges in the mechanical and material fields [2].

The HP Multi Jet Fusion™ technology, henceforth MJF, was designed to embrace the market niche for both functional prototyping and end-part manufacturing in the industrial field. MJF is able to achieve similar results to plastic transformation processes such as plastic injection moulding. It is considered a High Speed Sintering (HSS) technology [3] as it involves the sintering of 2D profiles of layers of powder, similar to Binder Jetting (BJ) technology, without the need of a laser. The MJF printhead prints functional agents in precise locations onto the material to define the geometry of the part and its properties. It is capable of printing thirty million drops per second across the width of the printing space [4]. This leads to very accurate dimensional precision ( $\pm 0.2\%$ ) compared with other technologies [5]. The printing velocity, the dimensional precision and the high quality in printed parts, turns this novel technology into an interesting manufacturing system for AM solutions.

The aim of this study is to show how the MJF technology can embrace the fabrication of both functional prototype and small batch series under water pressures in liquid state. It is not allowed by other technologies, due to the lack in mechanical properties or the porosity structure of the material. There is a need in the fluid handling industry to manufacture parts resistant to pressure, maintaining their leak tightness through AM technologies. As for the requirement of tightness under fluid

pressure, the weak point is the porosity generated in the manufacturing process. Currently, coatings or infiltrations are required to seal the material and ensure no leakage through porosity [6].

Due to the nature of the process, technologies such as Fused Filament Fabrication (FFF) or Selective Laser Sintering (SLS) [7] create porosities located at the interface between the layers [8]. Moreover, the manufactured parts are not completely sealed and lead to alterations in their mechanical properties [7–9] even as a function of time [12]. Recent studies try to identify laser additive processing to functionality [13]. Even though the resulting parts from SLS are not entirely dense, very low degrees of porosity can be obtained by adjusting the printing parameters [14]. This porosity was created by defects in the sintering of the material, where some of the grains did not fuse, producing empty spaces in the subsequent cooling process [15]. Two types of porosities were created: irregular pores caused by shrinkage and non-fused parts and spherical pores that came from trapped gases or evaporation of the material [16].

On the other hand, technologies based on photosensitive resins such as Stereolithography (SLA) and Poly Jet (PJ) do not create porosities in their structure. Resins used are formed by acrylate groups, which help to reach a quick reaction, and epoxy groups that enhance mechanical properties to the material [16]. The main problem is that the liquid resins are not suitable for the manufacturing the final parts. The degradation of the material caused by aging directly affects the mechanical properties [13,14]. Photosensitive resins are not recommended as a final solution, although they are very useful in design phase [15-17]. In addition, these types of resins increase their volume in contact with water or moisture. For this reason, they cannot be used as the final product as they would lose all their manufacturing tolerances [18]. Recent studies focus on parameters to obtain a uniform deposition of material [20] with different additive manufacturing techniques.

Another issue is the sealing of the printed parts, which presents porosity in their structure. There are already existing solutions, where the choice of the solution depends on several factors such as cost, machinery, and process time, among others. The selected solution has a direct impact on the time spent per part and, consequently, its cost. Therefore, when the part is analysed and requires a sealing treatment, it is replaced by the conventional plastic transformation processes due to the high industrial cost [21]. The most used sealing methods in the additive manufacturing industry are [22]:

Painting and filling: When parts need only partially sealed surfaces, a few coats of paint and a little body putty can be an inexpensive option. Since this is a manual operation, the accuracy and quality of the product is influenced by the technician's skill and care. The advantages of this option include low cost, short cycle time and ease of application. Its disadvantages are the lack of an airtight seal and inability to resist high temperatures and chemicals.

Smoothing station: This method seals the surfaces of a part by exposing them to a vaporized smoothing agent inside a chamber. The smoothing station is very easy to use and preserves dimensional integrity [23]. Its use is limited to applications with pressures that do not exceed atmospheric pressure and temperatures equal to or below 100 °C. This technique only seals the surface holes but not the internal channels. If the sealing of the interior is required, it should be combined with a previous infiltration.

Solvent dipping: Dipping additive manufacturing parts in a solvent could be a substitute for the smoothing station, when it is unavailable or the part exceeds the chamber capacity. All the characteristics are the same as the smoothing station except the dimensional accuracy, which is lower. The solvent melting action is quick and aggressive, so dimensional accuracy is difficult to control. As with the smoothing station, the use of this method should be limited to low temperature and atmospheric pressure applications.

Adhesives coatings and infiltrations: They are substances based on epoxy formulation with different viscosities. Adhesives of high viscosity should be applied with a surface coating. In contrast, low viscosity infiltrations can be performed in vacuum chambers in order to ensure the adhesive enters to the interior of the part by controlling the necessary process time [24]. By applying adhesives to parts manufactured with SLS and FFF technologies, resistance to water pressure can only reach a value of 0.45 MPa [25].

The results reached in this work are important for the industry, because they show manufacturers the possibility of considering additive manufacturing as an alternative to traditional manufacturing methods. Specially to produce spare parts and small batches including mass customization for pressurized components. This paper is a novel approach to design and manufacture fluid handling components with additive manufacturing Multijetfusion technology avoiding the problems of water leakage. This problem is common in most of additive manufacturing technologies caused by porosity structures in the material.

## 2. Materials and Methods

The fabrication of a valve through MJF technology with PA12 is presented in this study. Specifically, a ball valve designed to isolate a liquid belonging to a conducting fluid system following the standard EN ISO 16135:2007 and the directive 97/23/EC. The valve is catalogued as PN10 (1 MPa). Nominal pressure (PN) is used as a reference of its mechanical resistance and corresponds to the maximum allowed water pressure at 20°C.

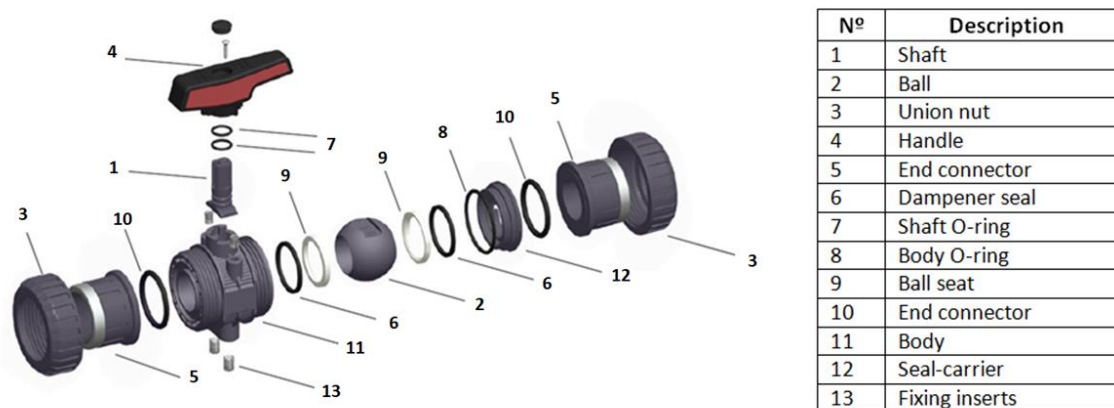


**Figure 1.** Exploded view of ball valve. Source:[21].

For the sake of simplicity, only the main parts of the valve (shell and union nuts) were considered to be printed with MJF (11 and 3, correspondingly, in Figure 1). These exterior coverage parts support two pressure origins: the pressure from the inner parts and the hygroscopic pressure.

The printed parts were evaluated with the same quality tests applied to an industrial production valve. It must satisfy the ISO 9393. This standard describes the method to verify the shell resistance under water pressure and the inner parts package effort. Together with the union nuts they must withstand the tensile strain caused by the water pressure inside the valve and comply with ISO 228-1.

The methodology used was divided in three stages. In the first stage, called fabrication process, the three-dimensional model has analysed. It was treated in the printing software. The thickness of the layer, the material used and the orientation of the parts in the space were set up. Before printing process, the material was subjected to a tensile test to correctly characterize its mechanical properties. Also, a fractography analysis was done to characterize the porous media. Furthermore, a leaks study was implemented by using a flowmeter, given different printing orientations and wall thickness for a range of pressure values. In the second stage, the physical dimensions of the parts were verified by using a three-dimensional scan. It compares their dimensions with the tolerances allowed in the production of the valves. In cases where tolerances are not satisfied, the machining of the parts must be done. The full valve assembly will be checked with a leak test using air as a fluid. The final stage is the product validation. It is determined whether the complete valve satisfies the quality standard for valves made of thermoplastic material.

An HP Jet Fusion 4200 machine was used to manufacture the parts of the valve. The printing parameters used were: 0.08 mm of layer height in the Z axis with a standard resolution of  $\pm 0.2\%$ . Balanced print mode was set up: one rolling step and two injection passes spending 10.5 sec per layer. Due to the shape of the parts, the cylindrical sections were oriented in the XY plain, where the resolution is highest. In XY plane orientation the step effect caused by an angular gradient lower than  $30^\circ$  in the Z axis is avoided.

Once manufactured, the parts were dimensionally analysed using a 3D scan (ATOX Scanbox). Then the set was assembled in order to validate the product. The next stage was identifying if there are any leakage points through the leak tester.

In this case, the shell test and the seat and packing test were studied. These tests provide information about the resistance and watertightness of the material. In order to carry on the tests there are some required restrictions shown below:

- Pressure appliances, as specified in the ISO 1167-1, have to be able to connect the sample and progressively apply water pressure following the standard of the product. It has to keep a constant pressure between +2 and -1% for the time specified in the ISO 9393-2, maintaining the temperature indicated in the product standard.
- Pressure calibrated sensor must be able to verify the test specified pressure without polluting the product.
- Thermometers must be able to verify the specified temperature in the assay.
- Timers have to be able to record the duration of the pressure application until the fail momentum during the trial time.

The procedure established for the shell test is as follows:

1. In the first place, the sample must be filled with water and conditioned for at least 1 hour at a temperature that does not deviate more than  $\pm 2^\circ\text{C}$  of the specified trial temperature.
2. Place the test sample in a mode that the entire valve body is under the trial pressure.
3. Make sure that the water temperature in the test tube is adjusted to the specific trial temperature.
4. Release any trapped air inside the trial sample.
5. Raise the pressure progressively until trial pressure specified in the ISO 9393-2 is reached, as fast as possible, but not in less than 30 seconds.
6. Keep the pressure and temperature duration specified in the standard ISO 9393-2.
7. Diminish the pressure until atmospheric pressure.

The ISO 9393-2 parameters of the trial according to the fabrication thermoplastic material are specified in detail. The polyamide material has not been included in the standard. Then the test parameters for the PVC-U, which is the original material of nut unions and shell as well as being the most restrictive case, were used. The shell test parameters are shown in Table 1.

**Table 1.** Shell test parameters for PVC-U material.

| Material | Minimum test time | Pressure test ( $P_{\text{test}}$ ) <sup>1</sup> | Design Stress ( $\sigma$ ) <sup>2</sup> | Assembly Stress ( $\sigma_s$ ) <sup>3</sup> | Temperature              | Inner fluid | Outer fluid  |
|----------|-------------------|--|---|---|--------------------------|-------------|--------------|
| PVC-U    | 1 hour            | 4.2 MPa  | 42 MPa                                  | 10 MPa                                      | $20 \pm 2^\circ\text{C}$ | Water       | Water or Air |

<sup>1</sup> The test pressure is measured following the formula:  $P_{\text{test}} = (\sigma_t / \sigma_s)$ .

<sup>2</sup> Design stress corresponds to the maximum stress for the elastic limit not to be exceeded avoiding its plastic strain (MPa).

<sup>3</sup> Stress induced under the assembly conditions (MPa).

The procedure established for the seat and packing test is specified below:

1. Firstly, the sample must be filled with water and conditioned for at least 1 hour at a specified temperature, which does not deviate more than  $\pm 2^{\circ}\text{C}$ .
2. Fully closed valve test:
  - a. Connect one end of the sample to the pressure line and the other end to a device capable of detecting leakage.
  - b. Fill the closed sample with the test fluid at the specified temperature.
  - c. Release any trapped air from the test sample.
  - d. Close the valve with the closing torque specified in the product standard.
  - e. Increase the pressure gradually until reaching the test pressure specified in ISO 9393-2, but not in less than 30 s.
  - f. Maintain the pressure and temperature duration specified in ISO 9393-2.
  - g. Check the seat tightness.
  - h. Reduce the pressure to atmospheric pressure.
3. Valve test totally or partially open:
  - a. Open the valve to such an extent that all related cavities and packings are under the test pressure.
  - b. Connect one end to the pressure supply and close the other end.
  - c. Fill the sample with the test fluid to the specified temperature and then close the flow downstream of the test sample.
  - d. Release any trapped air from the test sample.
  - e. Increase the pressure gradually until reach the test pressure specified in ISO 9393-2, but not in less than 30 s.
  - f. Maintain the pressure and temperature duration specified in ISO 9393-2.
  - g. Check the body and packing tightness.
  - h. Reduce the pressure to atmospheric pressure.

The procedure determined for seat and packing test and the corresponding parameters are specified in detail in the ISO 9393-2 and they are shown in Table 2.

**Table 2.** Seat and packing test parameters.

| Test                      | Test minimum time    | Test pressure ( $P_{\text{test}}$ ) | Temperature                   | Inner fluid | Outer fluid |
|---------------------------|----------------------|-------------------------------------|-------------------------------|-------------|-------------|
| Seat test (close valve)   | DN $\leq$ 200 = 15 s | 1.1 MPa                             | 20 $\pm$ 2 $^{\circ}\text{C}$ | Water       | Air         |
| Packing test (open valve) | DN $>$ 50 = 30 s     | 1.5 MPa                             | 20 $\pm$ 2 $^{\circ}\text{C}$ | Water       | Air         |

### 3. Results

#### 3.1. Tensile tests

Tensile tests were carried out on specimens ASTM D638 Type I. They were manufactured on three different printing directions obtaining stress versus strain curves. For each orientation, three specimens were tested. Results from such tensile tests are shown in Figure 2.

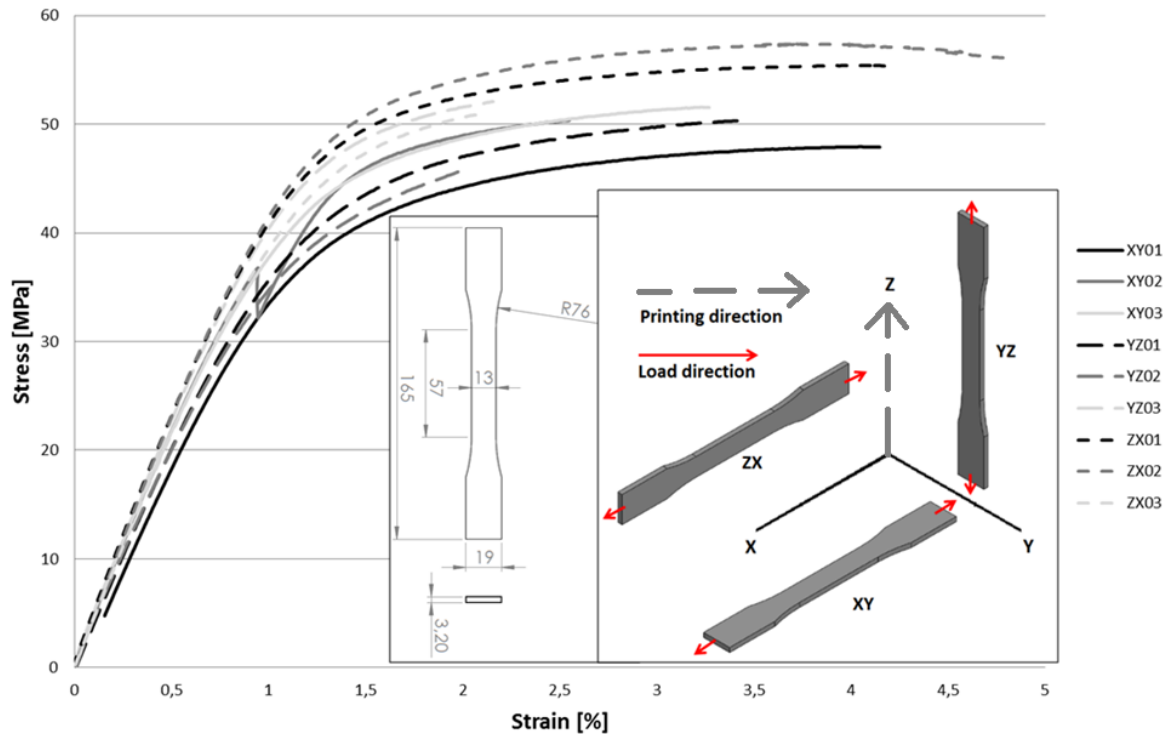


**Figure 2.** Tensile tests for several fabrication directions using D638 Type I specimens.

The mechanical properties were obtained from the tensile test curves. Furthermore, a comparison between these measurements and reference values of polyamide resins and vinyl compounds are provided in Table 3.

**Table 3.** Values obtained from tensile tests and reference values from russian GOST normative 10589-63.

| Specimen            | E (MPa)   | $\sigma_y$ (MPa) | $\sigma_m$ (MPa) | $\epsilon_r$ (%) |
|---------------------|-----------|------------------|------------------|------------------|
| XY01                | 3525      | 33.5             | 47.9             | 4.1              |
| XY02                | 4202      | 35.2             | 50.3             | 2.5              |
| XY03                | 4087      | 37.7             | 51.6             | 3.3              |
| YZ01                | 3817      | 35.5             | 50.3             | 2.5              |
| YZ02                | 3767      | 34.6             | 45.6             | 2.0              |
| YZ03                | 4321      | 40.4             | 52.1             | 2.2              |
| ZX01                | 4391      | 41.5             | 55.4             | 4.2              |
| ZX02                | 4409      | 41.4             | 57.4             | 4.8              |
| ZX03                | 4106      | 40.1             | 50.9             | 2.1              |
| PA (GOST 10589-63)  | 1167      | -                | 49.0-58.8        | 100              |
| PVCU (GOST 9639-61) | 2942-3923 | -                | 39.2-58.8        | 10-100           |

According to Galileo-Leibnitz, also known as Clebsch-Rankine criteria [26], the maximum stress is calculated. The maximum stress for polyamides, according to Russian GOST normative 10589-63, is within the range of 49-59 MPa approximately. Experimental results range obtained were 48-57 MPa. There is not a clear relation between fabrication direction and maximum stress. The observed rupture for all fabrication directions was cohesive and fragile with ultimate strain lower than 5% in all cases.

In addition, an Analysis of Variances (ANOVA) test was performed taking into account the maximum stress for the three populations: XY, YZ and ZX. The obtained results showed that there is no strong evidence to reject the null hypothesis, which considers that all the specimens belong to the same population, as the obtained p-value was 0.135. However, this result was partly expected due to the low number of specimens for each population.

### 3.2. Leaking and pressure tests

Leak tests were carried out with vessel samples made of PA12 with horizontal (H) and vertical (V) printing orientations. The inner diameter was a constant parameter (25 mm) for all the samples, the wall thickness being the parameter to be modified, ranging from 0.4 mm to 0.7 mm. The wall thickness was only modified in the cylindrical zone with a length of 50 mm. All tests were performed using a flowmeter to measure leaks at different pressures, up to 0.4 MPa.

Test results show that, for samples printed with the same orientation, lower thickness leads to higher leak values. On the other hand, for samples with same wall thickness, the orientation has great impact on the leak values, the vertical orientation being the most critical. It is related to the number of layers and the air gaps that can form during the printing process. Concerning the printing height, the number of layers is greater with the vertical orientation; therefore, the probabilities of air gaps forming during the printing process are higher. Figure 3 shows the design of the samples, as well as the leak values at different pressures.

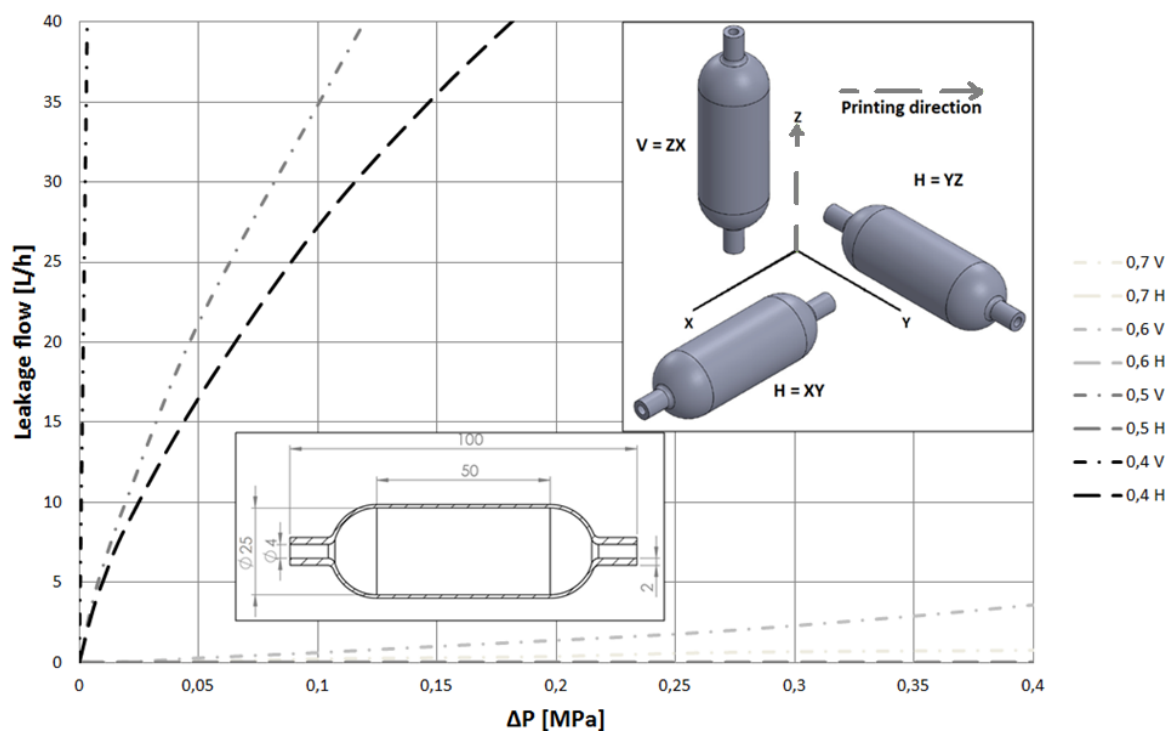


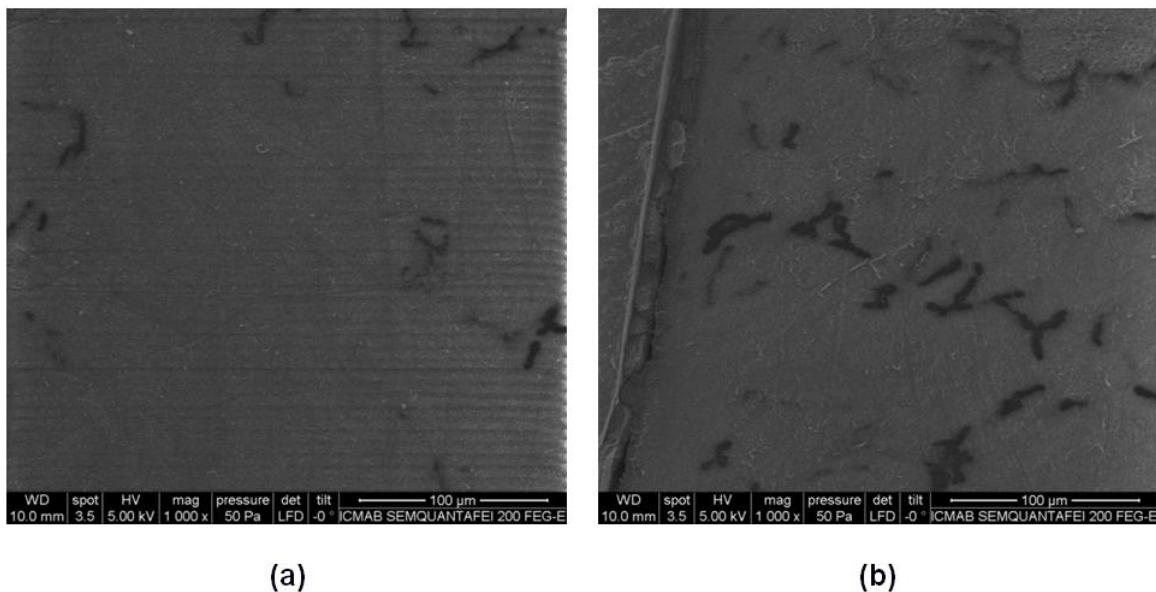
**Figure 3.** Leakage flow rate and pressure drop for all specimens.

For a leak value of 3 l/h the pressure drops ( $\Delta P$ ) values have been calculated in the Table 4. It shows that both printing orientation and thickness are significant variables that affect leakage values.

**Table 4.** Pressure drop for a leak value of 3 l/h.

| Thickness (mm) | Printing orientation (H=horizontal or V=vertical) | Pressure to leak 3l/h (MPa) |
|----------------|---|-----------------------------|
| 0.7            | V   | >0.400                      |
| 0.7            | H   | >0.400                      |
| 0.6            | V   | 0.357                       |
| 0.6            | H   | >0.400                      |
| 0.5            | V   | 0.044                       |
| 0.5            | H   | >0.400                      |
| 0.4            | V   | 0.003                       |
| 0.4            | H   | 0.052                       |

This information is relevant for design engineers during the design phase. The design rules presented are very useful to make decisions about the dimension and printing strategy of the pressurized component. In Figure 4 two samples with different orientations, but with the same wall thickness, are sectioned and visually inspected through a fractography analysis. The quantity of pores found in the vertical orientation is much higher. It was concluded that the printing orientation plays a significant role in the creation of pores and consequently in the leakage.

**Figure 4.** (a) SEM in XY orientation, (b) and YZ orientation.

### 3.3. Tolerances on final parts

The geometrical tolerances of all fabricated parts were checked and the distribution curves were obtained. The expected results for the standard resolution of the machine were satisfactory. Both parts were adequate in terms of tolerances with the dimensions varying between  $\pm 0.3$  mm. For this dimension range, machining of the parts was not necessary.

### 3.4. Shell test on final assembly

A pressure study was required prior to shell test on the final assembly. Depending on the printing orientation, the efforts required for the part are different. In XY and YZ orientation, or horizontal direction, the stress applied during the trial is shown in formula 1.

$$\sigma \cdot 2 \cdot t = P \cdot 2 \cdot r \rightarrow \sigma_{XY/YZ} = \frac{P \cdot r}{t} \quad (1)$$

Where:

$\sigma$ = stress [MPa],  $t$ = thickness [mm],  $r$ = radius [mm],  $P$ =pressure [MPa]

In ZX orientation, or vertical direction, the stress applied during the trial is shown in formula 2.

$$\sigma \cdot 2 \cdot \pi \cdot r \cdot t = P \cdot \pi \cdot r^2 \rightarrow \sigma_{ZX} = \frac{P \cdot r}{2 \cdot t} \quad (1)$$

In this case, the cylindrical section was oriented in the XY plane, where the resolution is higher. In this trial, the pressure increased exponentially until it reached the set point (4.2 MPa). Following formula 2, the total stress applied was 15.8 MPa. The security factor for PA12 is about 2.5. Therefore, there is no risk of explosion.

The pressure control system acts on the pump and the pressure multiplier to reduce the pressure until the set point. A stabilization time of thirty seconds was programmed. During this time, the pressure has increased, and the environment is stabilized to the set point. The one-hour test starts when pressure and temperature were constant. In this process, a non-significant pressure decrease is observed due to material expansion. It is placed in the elastic section, creating empty gaps and consequently diminishing the system pressure. Pressure deviations are not detected during the test process. The results were satisfactory as no type of leak or valve explosion were found in the sample. Figure 5 shows the time series of the pressure evolution. As to the seat and packing assembly, the results have been satisfactory in that no leakage is observed through the valve seat and packing during the trial time, as shown in Figure 5. In both cases, there is noise in the pressure measurement during the trial test time due to the sensor. The variation is approximately  $\pm 3$  kPa.

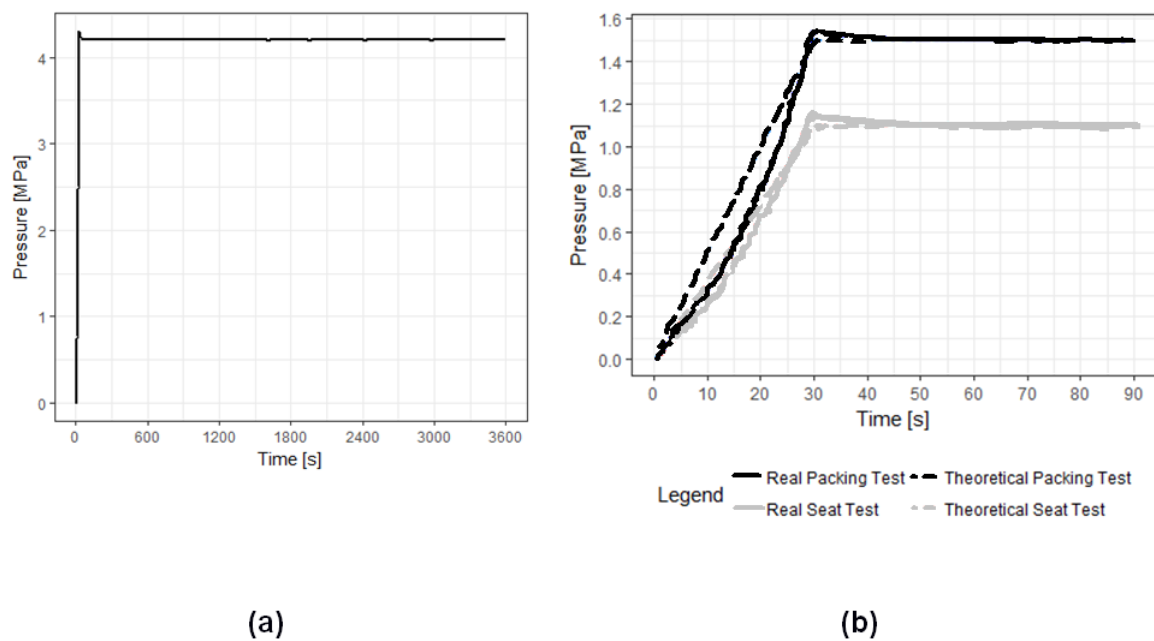


**Figure 5.** (a) Shell test results (b) Seat a packing test results..

#### 4. Conclusions

Considering the performed tests and the analysis of the results, several conclusions can be drawn:

1. The MJF technology can encompass the market niche for both the functional prototype and the end parts in the fluid handling field. This technology is able to substitute conventional plastic transformation methods, such as plastic injection moulding.
2. This solution avoids sealing of the printed parts as a post-process for achieving the desired functionality in the fluid conduction industry. The coating and infiltration seals only allow maximum pressures of 0.45 MPa whilst with MJF technology 4.2 MPa of water pressure was achieved for one hour, due to the lack of porosity in its structure.
3. Wall thickness and printing orientation are key variables which determine the watertightness of the samples. For the same wall thickness, vertical orientation requires higher number of layers to be printed, and therefore is more likely to have air gaps that lead to greater leak values. Test results show that for samples printed with the same orientation, a lower thickness leads to higher leak values.
4. Watertightness has been validated through a real case: an industrial ball valve. The tests under the standard pressures of the shell and packaging/seat have been satisfactory, showing no leaks and therefore comply with the quality control specified for PN10 ball valves made with thermoplastic material.

**Author Contributions:** “Conceptualization, Garcia-Granada and Morales-Planas; Methodology, Travieso-Rodriguez; Tensile tests, Lluma-Fuentes; Fabrication, Morales-Planas and Minguella-Canela; Formal Analysis, Travieso-Rodriguez and Garcia-Granada; Investigation, Morales-Planas; Resources, Morales-Planas; Writing-Original Draft Preparation, Morales-Planas and Garcia-Granada;

**Funding:** This work was supported by Generalitat de Catalunya [2015 DI 029].

**Conflicts of Interest:** The authors declare no conflict of interest.

#### References

1. G. Gomez-Gras, R. Jerez-Mesa, J. A. Travieso-Rodriguez, and J. Lluma-Fuentes, “Fatigue performance of fused filament fabrication PLA specimens,” *Mater. Des.*, vol. 140, pp. 278–285, 2018.
2. S. C. Ligon, R. Liska, J. Stampfl, M. Gurr, and R. Mülhaupt, “Polymers for 3D Printing and Customized Additive Manufacturing,” *Chemical Reviews*, vol. 117, no. 15, pp. 10212–10290, 2017.
3. N. Hopkinson and P. Erasenthiran, “High speed sintering - early research into a new rapid manufacturing process,” *Solid Free. Fabr. Symp. Proc.*, pp. 312–320, 2004.
4. R. Goodridge and S. Ziegelmeier, “Powder bed fusion of polymers,” in *Laser Additive Manufacturing: Materials, Design, Technologies, and Applications*, 2016, pp. 181–204.
5. G. D. Kim and Y. T. Oh, “A benchmark study on rapid prototyping processes and machines: quantitative comparisons of mechanical properties, accuracy, roughness, speed, and material cost,” *Proc. Inst. Mech. Eng. Part B J. Eng. Manuf.*, vol. 222, no. 2, pp. 201–215, Oct. 2008.
6. M. Schmid and G. Levy, “Lasersintermaterialien – aktueller Stand und Entwicklungspotential,” *Addit. Fert. - vom Prototyp zur Ser.*, pp. 43–55, 2009.
7. K. G. Cooper, *Rapid prototyping technology*, vol. 200. Marcel Dekker New York, 2001.
8. J. Gardan, “Additive manufacturing technologies: state of the art and trends,” *Int. J. Prod. Res.*, vol. 54, no. 10, pp. 3118–3132, 2016.
9. M. Domingo-Espin, S. Borros, N. Agullo, A.-A. Garcia-Granada, and G. Reyes, “Influence of Building Parameters on the Dynamic Mechanical Properties of Polycarbonate Fused Deposition Modeling Parts,” *3D Print. Addit. Manuf.*, vol. 1, no. 2, pp. 70–77, 2014.

10. M. Domingo-Espin, J. M. Puigoriol-Forcada, A. A. Garcia-Granada, J. Llumà, S. Borros, and G. Reyes, "Mechanical property characterization and simulation of fused deposition modeling Polycarbonate parts," *Mater. Des.*, vol. 83, pp. 670–677, 2015.
11. B. Shaw and S. Dirven, "Investigation of porosity and mechanical properties of nylon SLS structures," in *Mechatronics and Machine Vision in Practice (M2VIP), 2016 23rd International Conference on*, 2016, pp. 1–6.
12. A. G. Salazar-Martín, M. A. Pérez, A. A. García-Granada, G. Reyes, and J. M. Puigoriol-Forcada, "A study of creep in polycarbonate fused deposition modelling parts," *Mater. Des.*, vol. 141, pp. 414–425, 2018.
13. T. Borkar, R. Conteri, X. Chen, R. V Ramanujan, and R. Banerjee, "Laser additive processing of functionally-graded Fe--Si--B--Cu--Nb soft magnetic materials," *Mater. Manuf. Process.*, vol. 32, no. 14, pp. 1581–1587, 2017.
14. J. A. Choren, S. M. Heinrich, and M. B. Silver-Thorn, "Young's modulus and volume porosity relationships for additive manufacturing applications," *Journal of Materials Science*, vol. 48, no. 15, pp. 5103–5112, 2013.
15. D. K. Leigh, "a Comparison of Polyamide 11 Mechanical Properties Between Laser Sintering and Traditional," *Int. Solid Free. Fabr. Symp.*, pp. 574–605, 2012.
16. D. Bourell, J. P. Kruth, M. Leu, G. Levy, D. Rosen, A. M. Beese, and A. Clare, "Materials for additive manufacturing," *CIRP Ann.*, vol. 66, no. 2, pp. 659–681, 2017.
17. S. Mansour, M. Gilbert, and R. Hague, "A study of the impact of short-term ageing on the mechanical properties of a stereolithography resin," *Mater. Sci. Eng. A*, vol. 447, no. 1–2, pp. 277–284, 2007.
18. K. Puebla, K. Arcaute, R. Quintana, and R. B. Wicker, "Effects of environmental conditions, aging, and build orientations on the mechanical properties of ASTM type I specimens manufactured via stereolithography," *Rapid Prototyp. J.*, vol. 18, no. 5, pp. 374–388, 2012.
19. X. Ottemer and J. S. Colton, "Effects of aging on epoxy-based rapid tooling materials," *Rapid Prototyp. J.*, vol. 8, no. 4, pp. 215–223, 2002.
20. [20] Q. Wu, J. Lu, C. Liu, X. Shi, Q. Ma, S. Tang, H. Fan, and S. Ma, "Obtaining uniform deposition with variable wire feeding direction during wire-feed additive manufacturing," *Mater. Manuf. Process.*, vol. 32, no. 16, pp. 1881–1886, 2017.
21. A. Pizzi and K. L. Mittal, *Handbook of adhesive technology*. CRC press, 2017.
22. I. Stratasys, *Technical application guide: Comparison of sealing methods for FDM materials*. 2015.
23. D. Espalin, F. Medina, K. Arcaute, B. Zinniel, T. Hoppe, and R. Wicker, "Effects of vapor smoothing on ABS part dimensions," in *Proceedings from Rapid 2009 Conference & Exposition, Schaumburg, IL*, 2009.
24. J. G. Zhou, M. Kokkengada, Z. He, Y. S. Kim, and A. a Tseng, "Low temperature polymer infiltration for rapid tooling," *Mater. Des.*, vol. 25, no. 2, pp. 145–154, 2004.
25. J. Mireles, A. Adame, D. Espalin, F. Medina, R. Winker, T. Hoppe, B. Zinniel, and R. Wicker, "Analysis of sealing methods for FDM-fabricated parts," in *Proceeding from Solid Free-form Fabrication Symposium*, 2011, pp. 185–196.
26. V. Pisarenko, G., Yakovlev, A. & Matviev, *Manual de resistencia de materiales*, First. Mir Moscú, 1985.